



The Abdus Salam
International Centre for Theoretical Physics



2253-6

**Workshop on Synergies between Field Theory and Exact Computational
Methods in Strongly Correlated Quantum Matter**

24 - 29 July 2011

**Field theories of Pure and Doped 2-D Quantum Antiferromagnets and High-Precision
Tests Based on Quantum Monte Carlo**

U.-J. Wiese

*Albert Einstein Center for Fundamental Physics
Institute for Theoretical Physics
Bern University
Bern, Switzerland*

Field theories of Pure and Doped 2-D Quantum Antiferromagnets and High-Precision Tests Based on Quantum Monte Carlo

Uwe-Jens Wiese

Albert Einstein Center for Fundamental Physics

Institute for Theoretical Physics, Bern University

Workshop on
Synergies between Field Theory and
Exact Computational Methods in
Strongly Correlated Quantum Matter

July 26, 2011

Key collaborator: Fu-Jiun Jiang (NTNU Taipei)



Outline

Cuprate Superconductors and Antiferromagnets

Correspondences between QCD and Antiferromagnetism

Quantum Heisenberg Model and Magnon Effective Field Theory

Hubbard Model and Effective Field Theory for Magnons and Holes

Two-Hole States Bound by Magnon Exchange

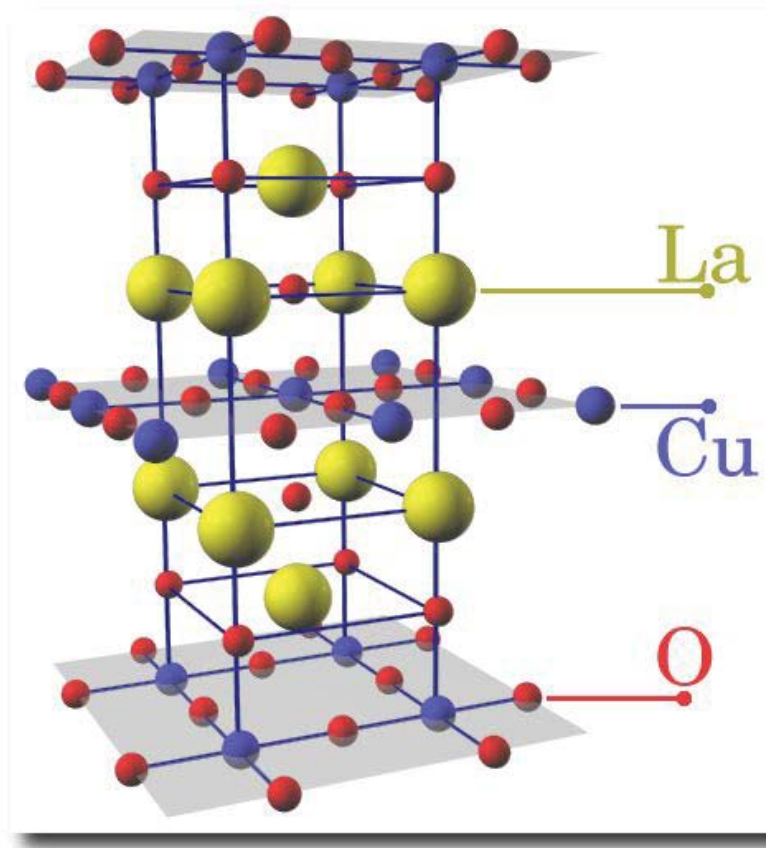
Holes Localized on a Skyrmion

From Graphene to $\text{Na}_x\text{CoO}_2 \cdot y\text{H}_2\text{O}$

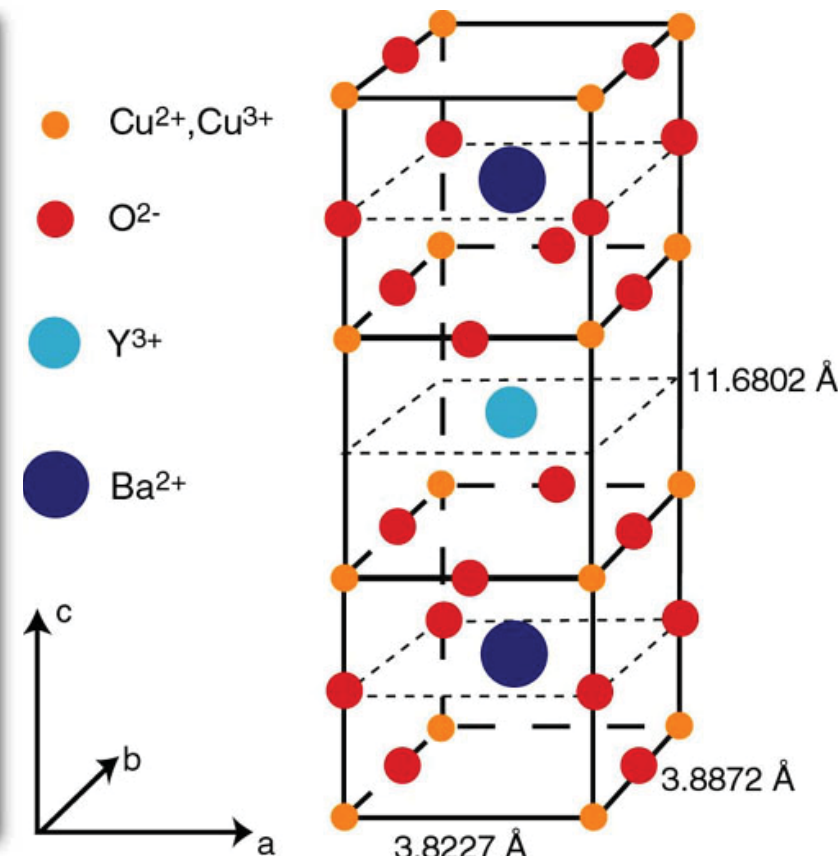
Outline

Cuprate Superconductors and Antiferromagnets

Antiferromagnetic precursors of high- T_c superconductors

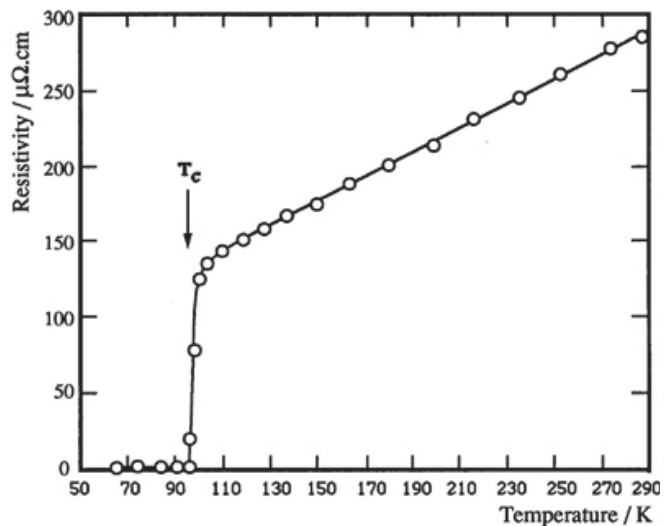
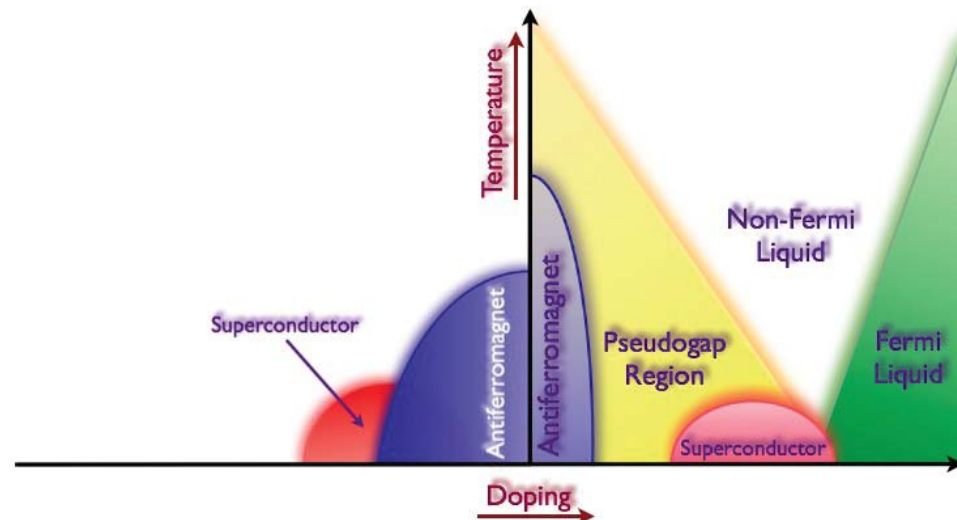
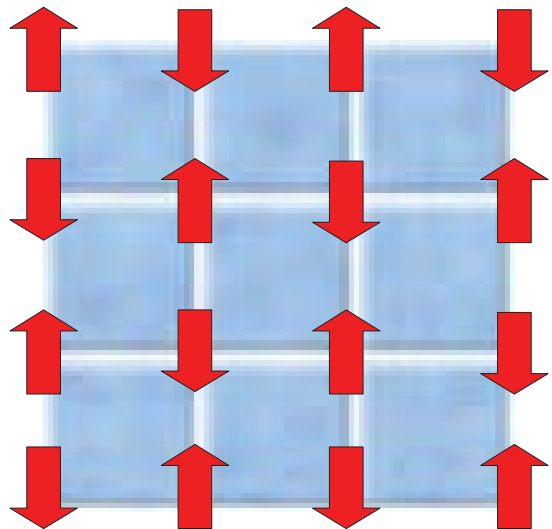


LaCuO



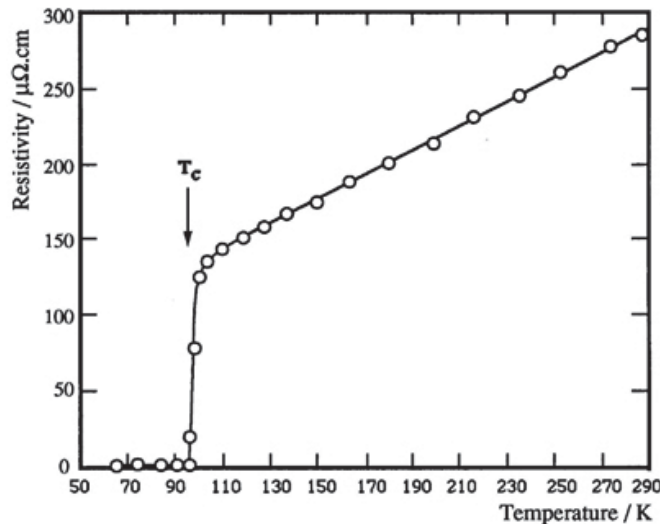
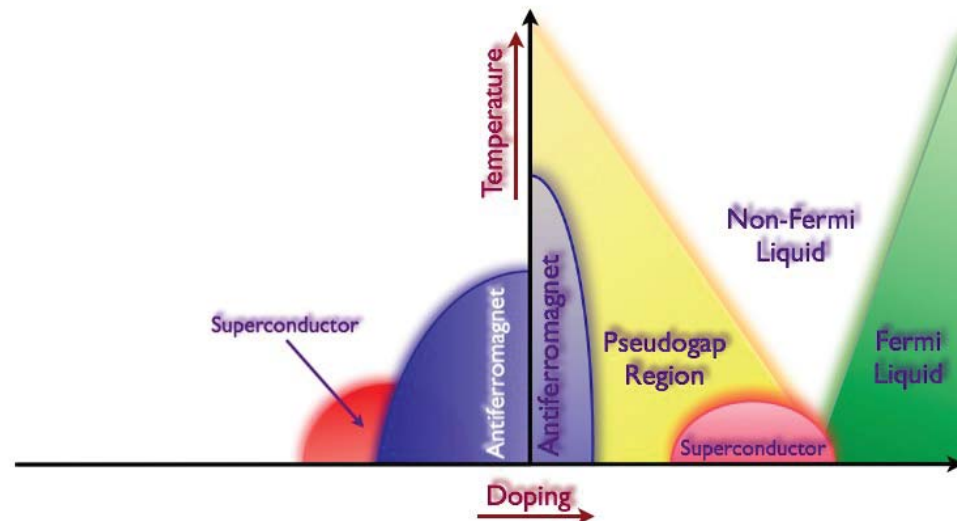
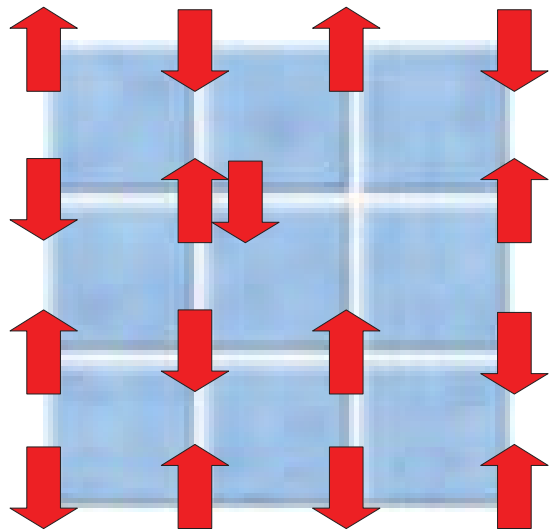
YBaCuO

Properties of cuprates



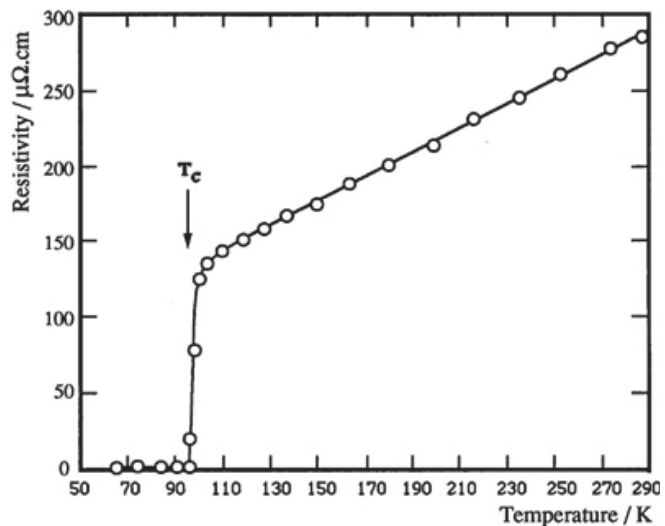
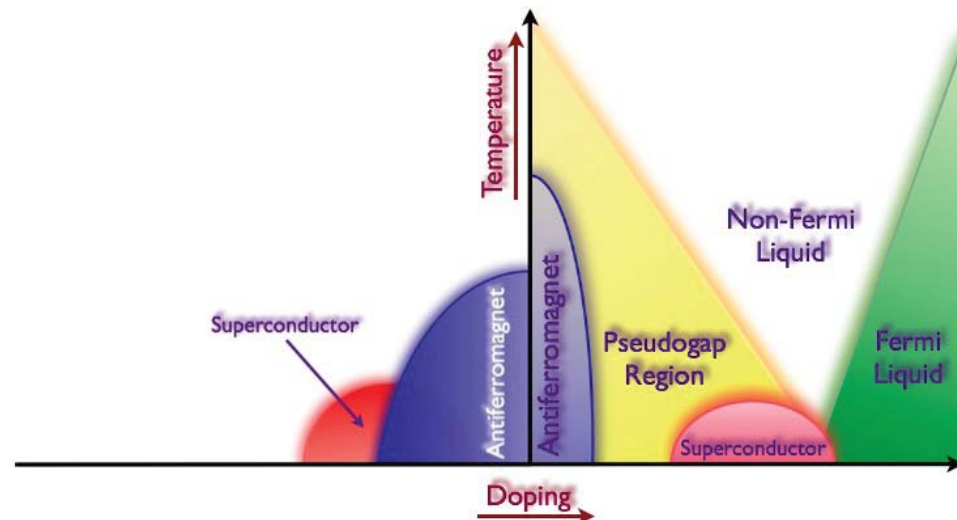
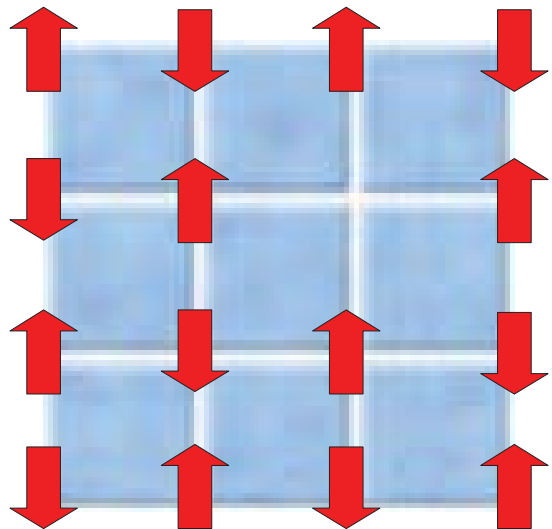
Temperature-dependence of resistivity

Properties of cuprates



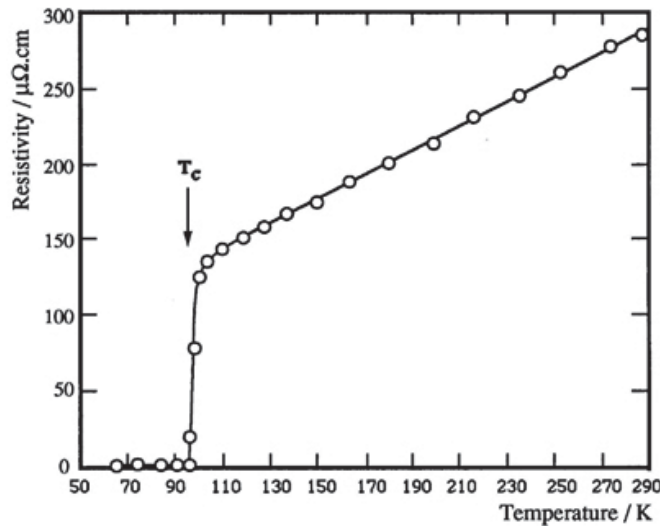
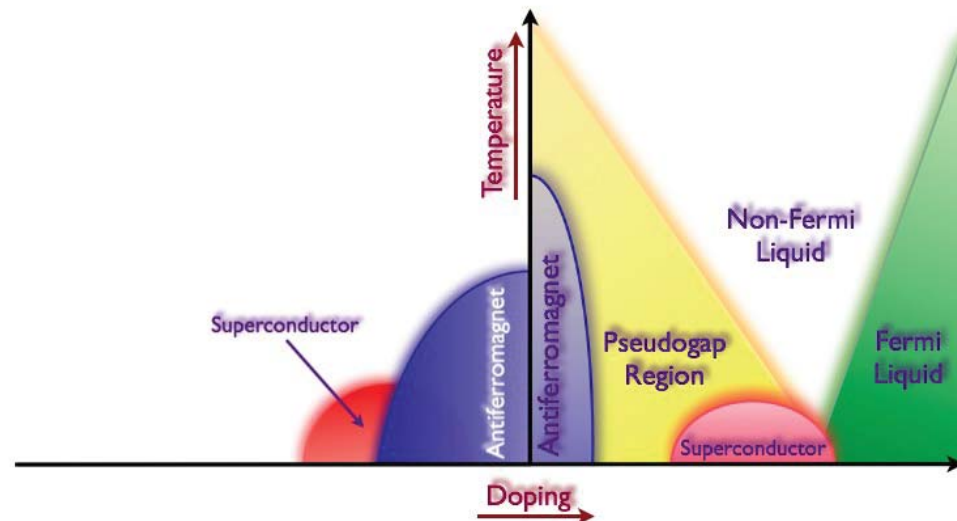
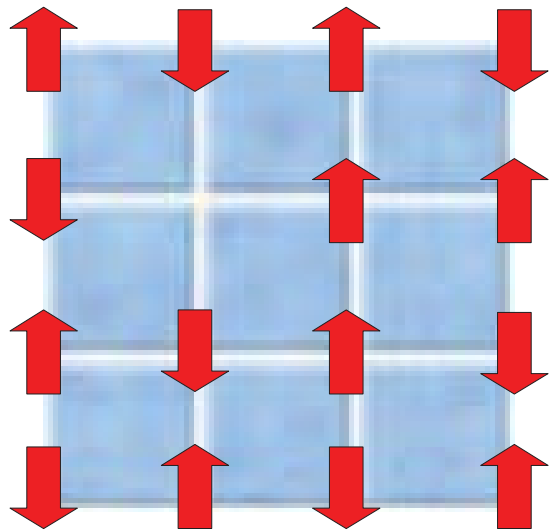
Temperature-dependence of resistivity

Properties of cuprates



Temperature-dependence of resistivity

Properties of cuprates



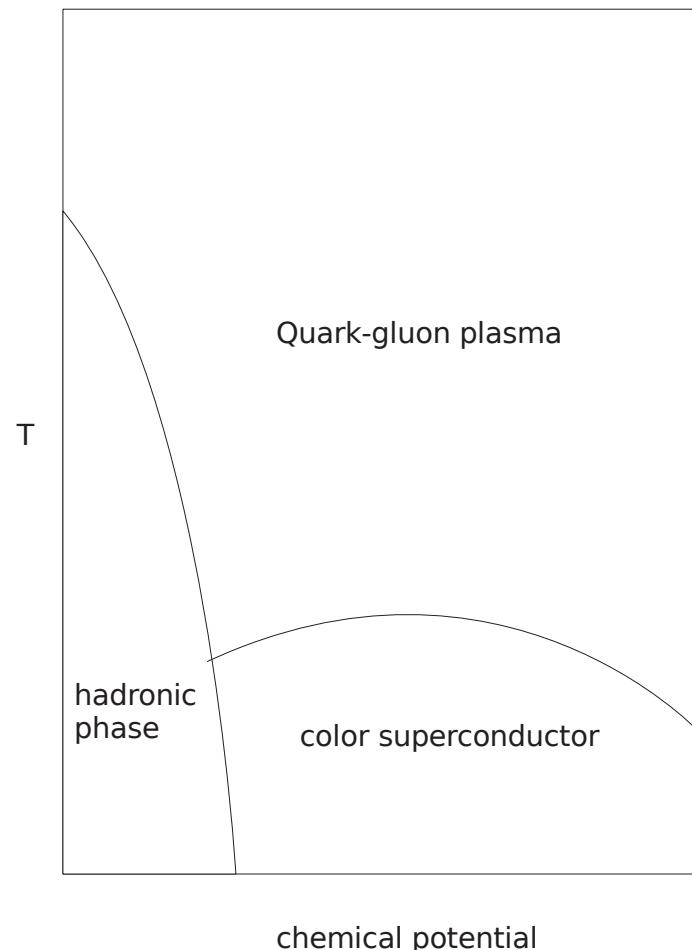
Temperature-dependence of resistivity

Outline

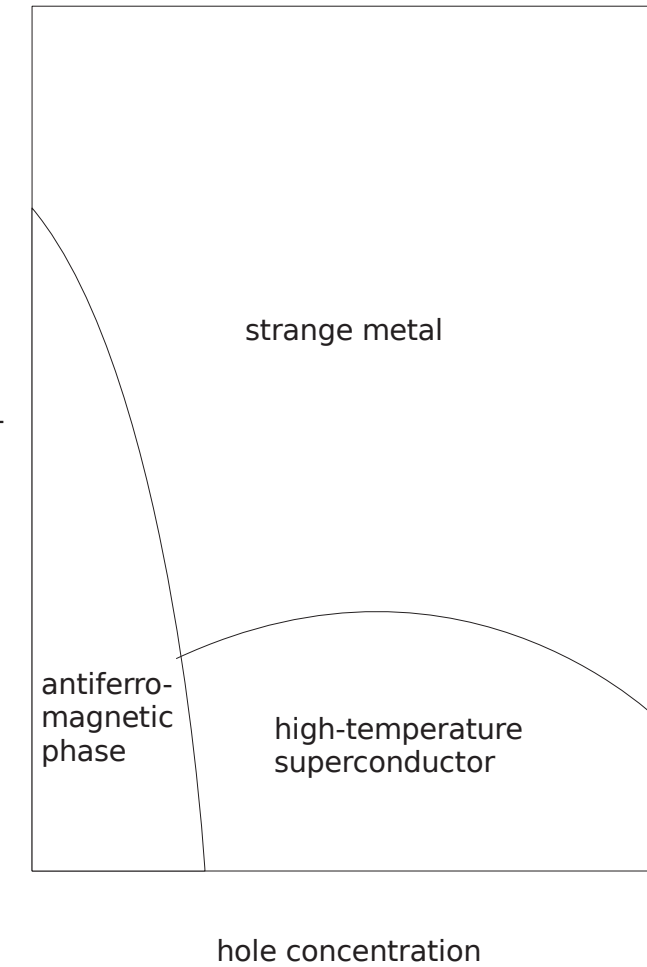
Correspondences between QCD and Antiferromagnetism

Phase diagrams of QCD and of doped antiferromagnets

QCD phase diagram



Phase diagram of cuprates



Correspondences between QCD and Antiferromagnetism

	QCD	Antiferromagnetism
broken phase	hadronic vacuum	antiferromagnetic phase
global symmetry	chiral symmetry	spin rotations
symmetry group G	$SU(2)_L \otimes SU(2)_R$	$SU(2)_s$
unbroken subgroup H	$SU(2)_{L=R}$	$U(1)_s$
Goldstone boson	pion	magnon
Goldstone field in G/H	$U(x) \in SU(2)$	$\vec{e}(x) \in S^2$
order parameter	chiral condensate	staggered magnetization
coupling strength	pion decay constant F_π	spin stiffness ρ_s
propagation speed	velocity of light	spin-wave velocity c
conserved charge	baryon number $U(1)_B$	electric charge $U(1)_Q$
charged particle	nucleon or antinucleon	electron or hole
long-range force	pion exchange	magnon exchange
dense phase	nuclear or quark matter	high- T_c superconductor
microscopic description	lattice QCD	Hubbard or t - J model
effective description of Goldstone bosons	chiral perturbation theory	magnon effective theory
effective description of charged fields	baryon chiral perturbation theory	magnon-hole effective theory

Outline

Quantum Heisenberg Model and Magnon Effective Field Theory

Quantum spins \vec{S}_x on a lattice with sites x

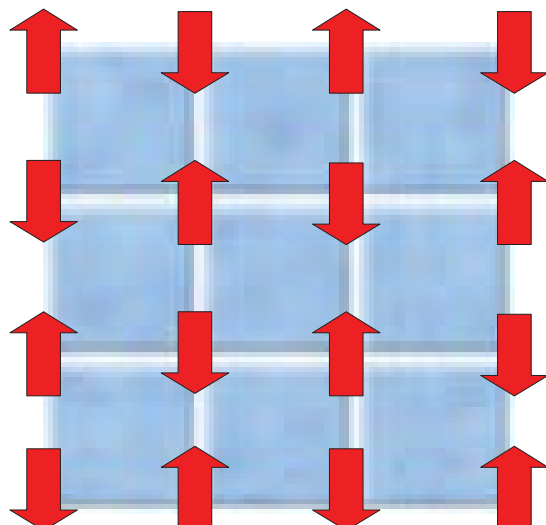
$$[S_x^a, S_y^b] = i\delta_{xy}\varepsilon_{abc}S_x^c, \quad \vec{S} = \sum_x \vec{S}_x$$

$SU(2)$ invariant Hamiltonian of the quantum Heisenberg model

$$H = J \sum_{\langle xy \rangle} \vec{S}_x \cdot \vec{S}_y, \quad [H, \vec{S}] = 0$$

Partition function at inverse temperature $\beta = 1/T$

$$Z = \text{Tr} \exp(-\beta H)$$



Staggered magnetization order parameter

$$\vec{M}_s = \sum_x (-1)^{(x_1+x_2)/a} \vec{S}_x$$

signals spontaneous symmetry breaking $SU(2) \rightarrow U(1)$

$$\frac{a^2}{L^2} |\langle \vec{M}_s \rangle| = \mathcal{M}_s \neq 0 \text{ at } T = 0$$

Magnon (Goldstone boson) field in $SU(2)/U(1) = S^2$

$$\vec{e}(x) = (e_1(x), e_2(x), e_3(x)), \quad \vec{e}(x)^2 = 1$$

Low-energy effective action for antiferromagnetic magnons

$$S[\vec{e}] = \int_0^\beta dt \int d^2x \frac{\rho_s}{2} \left(\partial_i \vec{e} \cdot \partial_i \vec{e} + \frac{1}{c^2} \partial_t \vec{e} \cdot \partial_t \vec{e} \right)$$

Chakravarty, Halperin, Nelson (1989)

Neuberger, Ziemann (1989)

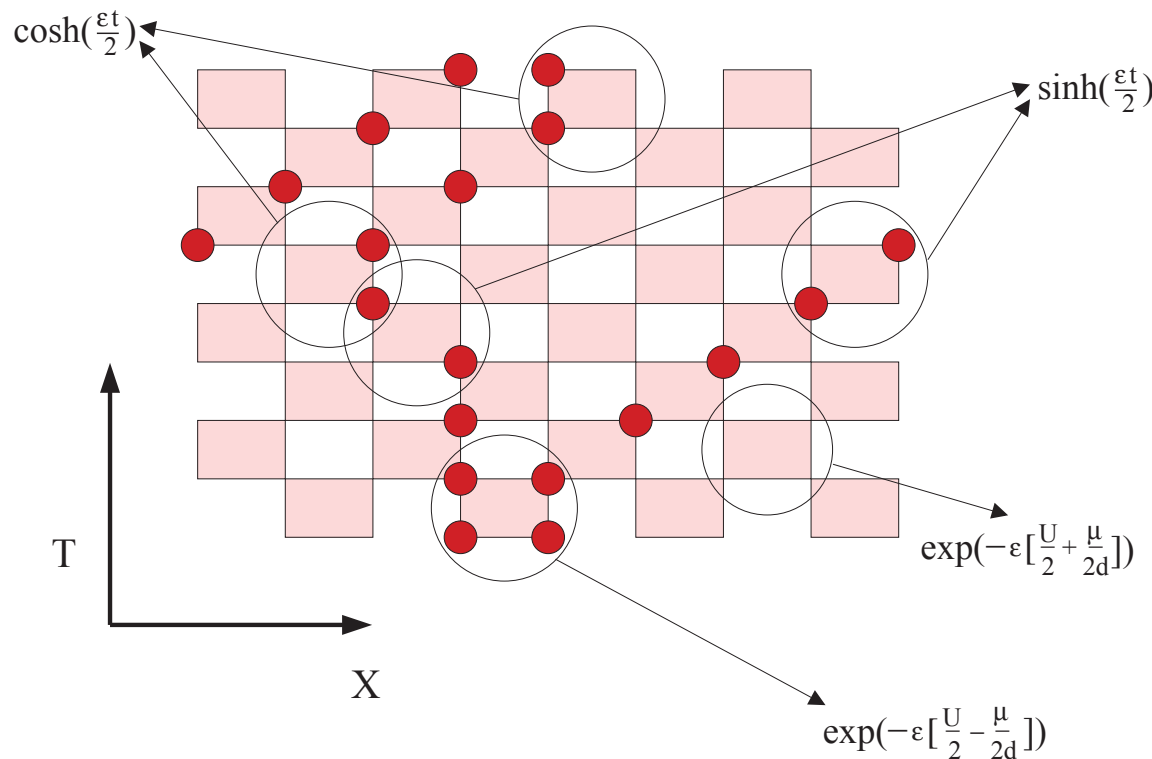
Hasenfratz, Leutwyler (1990)

Hasenfratz, Niedermayer (1993)

Chubukov, Senthil, Sachdev (1994)

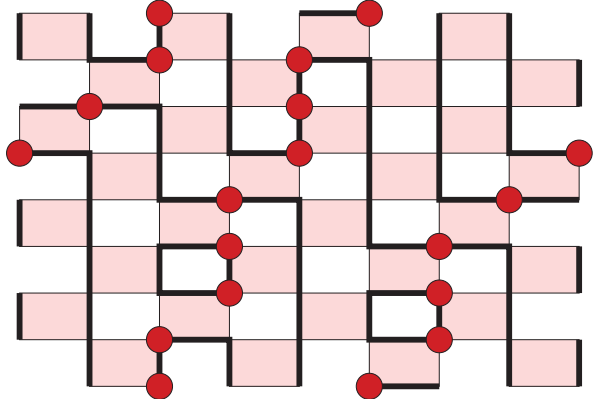
Path integral

$$\begin{aligned}
 Z &= \text{Tr}[\exp(-\varepsilon H_1) \exp(-\varepsilon H_2) \dots \exp(-\varepsilon H_M)]^N \\
 &= \sum_{[s]} \text{Sign}[s] \exp(-S[s])
 \end{aligned}$$



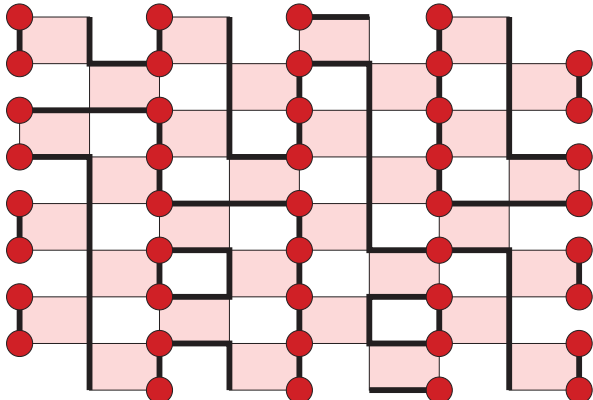
In this case: $M = 2$, $t = U = J$, $\mu = 0$.

Cluster decomposition



All spins in a cluster are flipped simultaneously with probability $\frac{1}{2}$.

Reference configuration



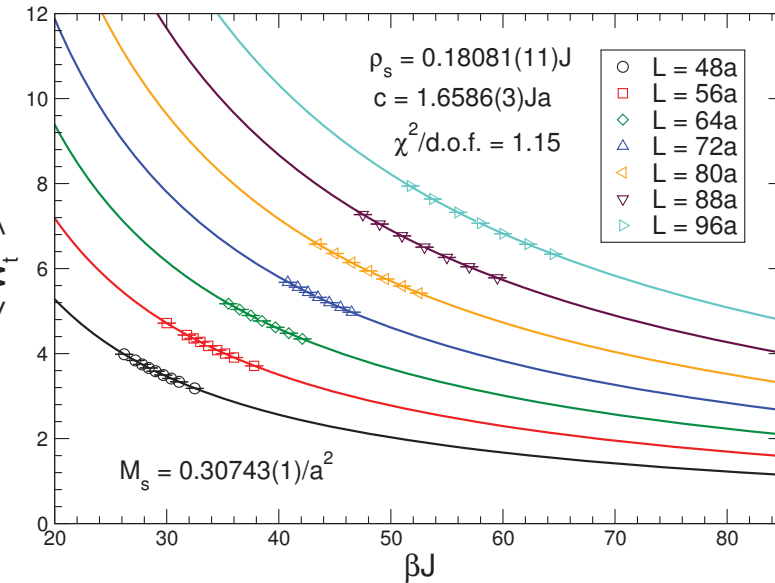
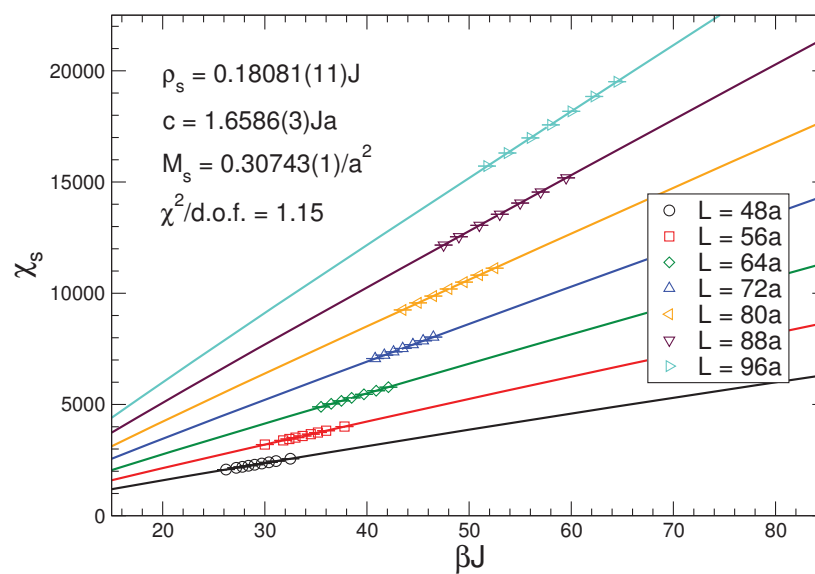
By appropriate cluster flips one can reach the classical Néel state.

Evertz, Lana, Marcu (1993); UJW, Ying (1994); Beard, UJW (1996)

Fit to analytic predictions of effective theory

$$\chi_s = \frac{\mathcal{M}_s^2 L^2 \beta}{3} \left\{ 1 + 2 \frac{c}{\rho_s L I} \beta_1(I) + \left(\frac{c}{\rho_s L I} \right)^2 [\beta_1(I)^2 + 3\beta_2(I)] \right\}$$

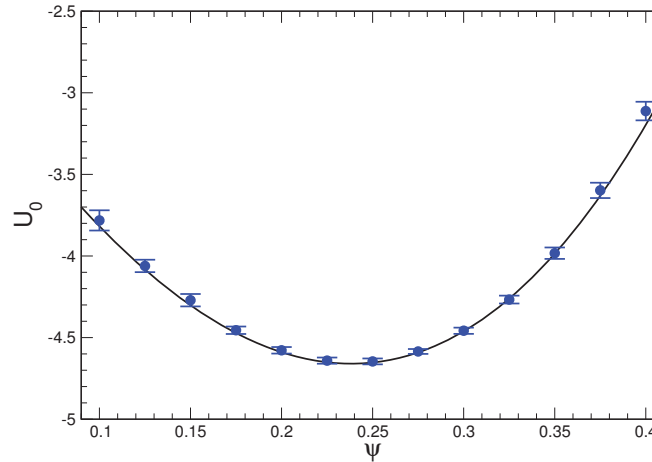
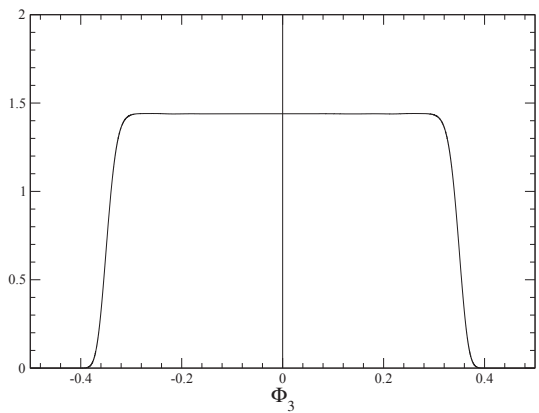
$$\chi_u = \frac{2\rho_s}{3c^2} \left\{ 1 + \frac{1}{3} \frac{c}{\rho_s L I} \tilde{\beta}_1(I) + \frac{1}{3} \left(\frac{c}{\rho_s L I} \right)^2 \left[\tilde{\beta}_2(I) - \frac{1}{3} \tilde{\beta}_1(I)^2 - 6\psi(I) \right] \right\}$$



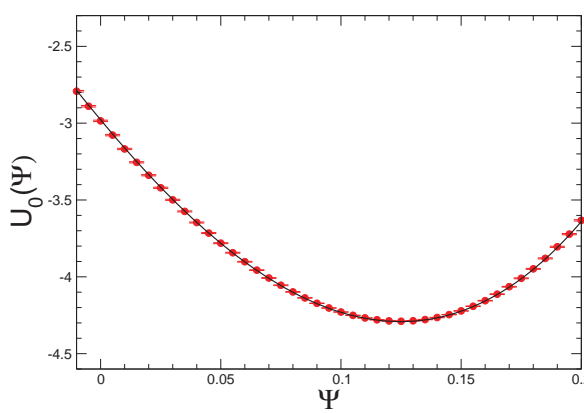
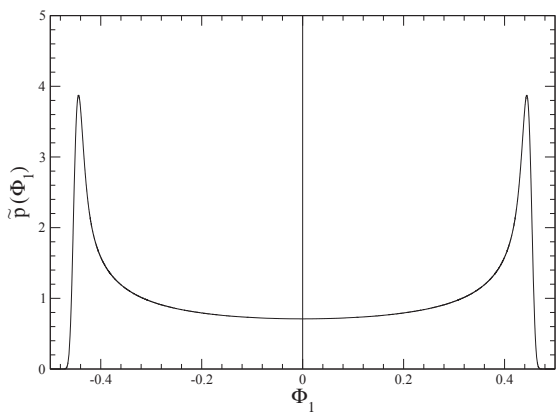
$$\mathcal{M}_s = 0.30743(1)/a^2, \quad \rho_s = 0.18081(11)J, \quad c = 1.6586(3)Ja$$

UJW, Ying (1994); Sandvik, Evertz (2010); Jiang, UJW (2010)

Excellent agreement with effective field theory predictions for the constraint effective potential: Göckeler, Leutwyler (1991)



Heisenberg model: Gerber, Hofmann, Jiang, Nyfeler, UJW (2009)
 XY model: Gerber, Hofmann, Jiang, Palma, Stebler, UJW (2011)



Jiang (2010) $\mathcal{M} = 0.43561(1)/a^2$, $\rho = 0.26974(5)J$, $c = 1.1348(5)Ja$

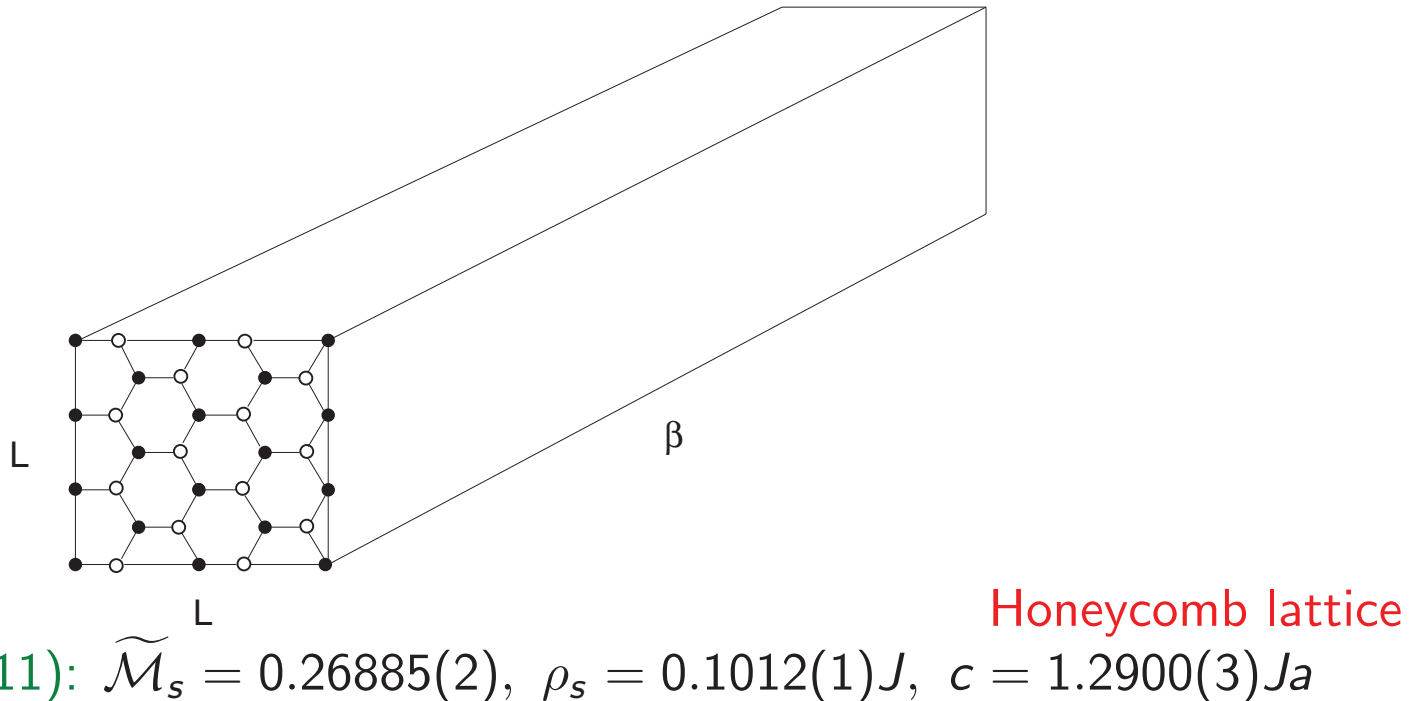
Effective rotor Lagrange function in the δ -regime $\beta c \gg L$

$$L = \int d^2x \frac{\rho_s}{2} \left(\partial_i \vec{e} \cdot \partial_i \vec{e} + \frac{1}{c^2} \partial_t \vec{e} \cdot \partial_t \vec{e} \right) = \frac{\Theta}{2} \partial_t \vec{e} \cdot \partial_t \vec{e}$$

Moment of inertia

$$\Theta = \frac{\rho_s L^2}{c^2} \left[1 + \frac{3.900265}{4\pi} \frac{c}{\rho_s L} + \mathcal{O}\left(\frac{1}{L^2}\right) \right]$$

Hasenfratz, Niedermayer (1993)



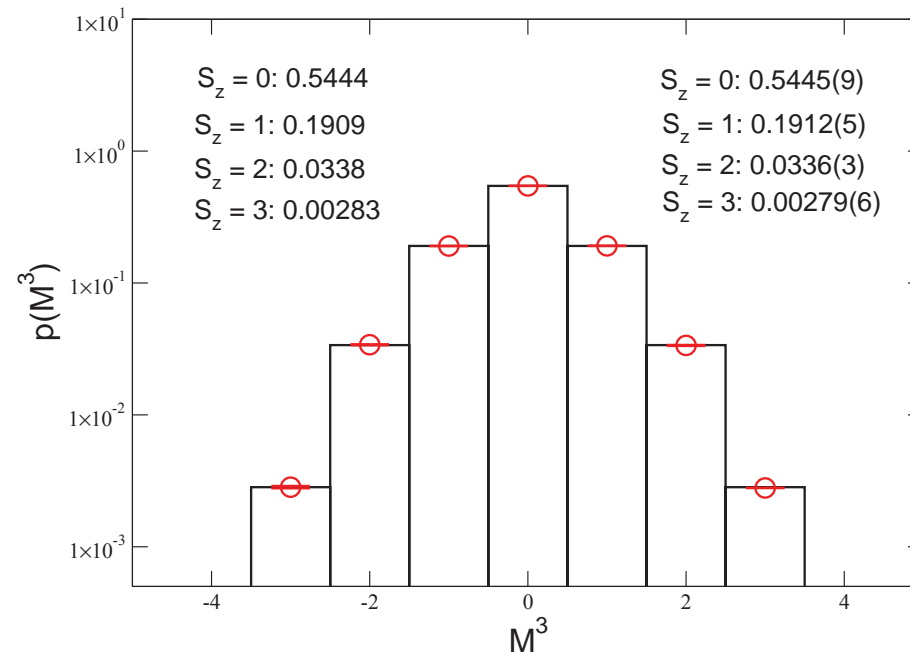
Rotor spectrum

$$E_S = \frac{S(S+1)}{2\Theta}$$

Probability distribution of magnetization $M^3 = S^3$

$$p(M^3) = \frac{1}{Z} \sum_{S \geq |M^3|} \exp(-\beta E_S), \quad Z = \sum_{S=0}^{\infty} (2S+1) \exp(-\beta E_S)$$

Honeycomb Lattice, 836 Spins, $\beta J = 60$



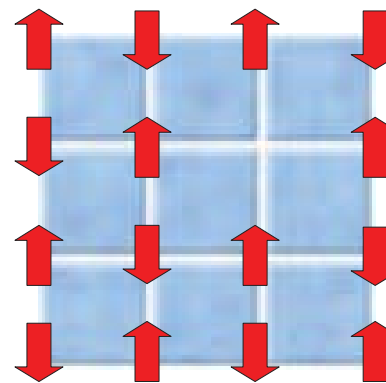
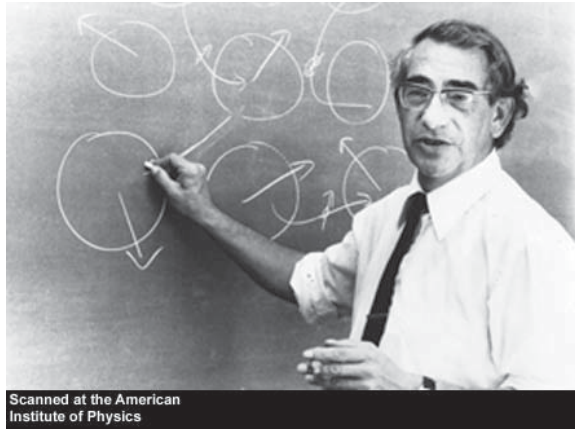
Perfect agreement without any adjustable parameters.

Jiang, Kämpfer, Nyfeler, UJW (2008)

Outline

Hubbard Model and Effective Field Theory for Magnons and Holes

The Hubbard Model



$$H = -t \sum_{\langle xy \rangle} (c_x^\dagger c_y + c_y^\dagger c_x) + U \sum_x (c_x^\dagger c_x - 1)^2, \quad c_x = \begin{pmatrix} c_{x\uparrow} \\ c_{x\downarrow} \end{pmatrix}$$

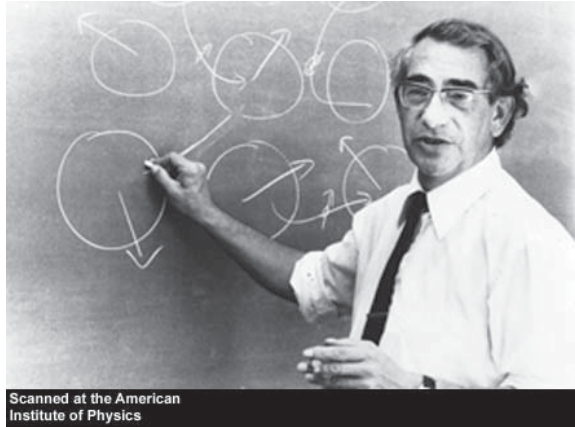
For large repulsion U it reduces to the t - J model

$$H = P \left\{ -t \sum_{\langle xy \rangle} (c_x^\dagger c_y + c_y^\dagger c_x) + J \sum_{\langle xy \rangle} \vec{S}_x \cdot \vec{S}_y \right\} P$$

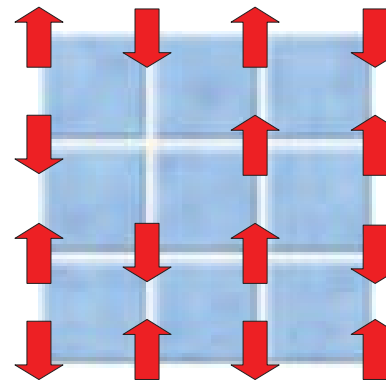
which further reduces to the Heisenberg model at half-filling

$$H = J \sum_{\langle xy \rangle} \vec{S}_x \cdot \vec{S}_y$$

The Hubbard Model



Scanned at the American
Institute of Physics



$$H = -t \sum_{\langle xy \rangle} (c_x^\dagger c_y + c_y^\dagger c_x) + U \sum_x (c_x^\dagger c_x - 1)^2, \quad c_x = \begin{pmatrix} c_{x\uparrow} \\ c_{x\downarrow} \end{pmatrix}$$

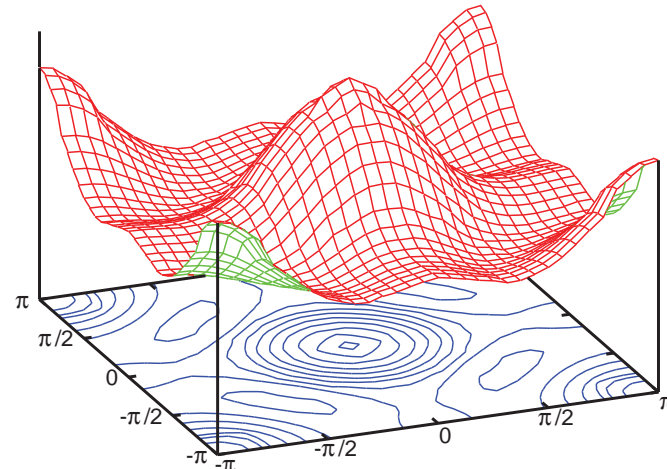
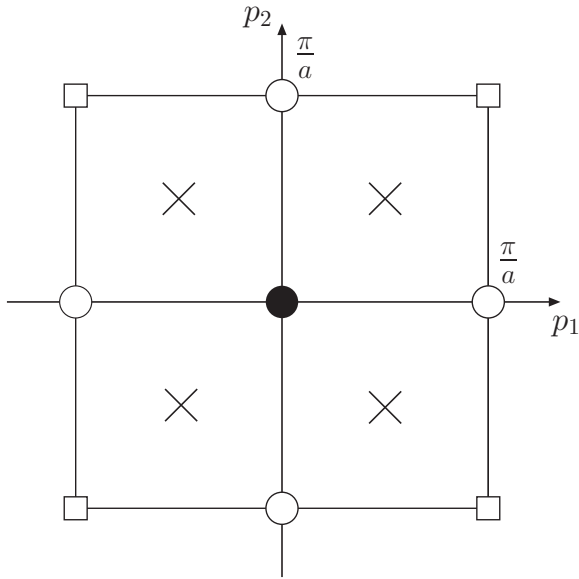
For large repulsion U it reduces to the t - J model

$$H = P \left\{ -t \sum_{\langle xy \rangle} (c_x^\dagger c_y + c_y^\dagger c_x) + J \sum_{\langle xy \rangle} \vec{S}_x \cdot \vec{S}_y \right\} P$$

which further reduces to the Heisenberg model at half-filling

$$H = J \sum_{\langle xy \rangle} \vec{S}_x \cdot \vec{S}_y$$

Hole dispersion in the t - J model



Hole pockets centered at lattice momenta

$$k^\alpha = \left(\frac{\pi}{2a}, \frac{\pi}{2a} \right), \quad k^{\alpha'} = -k^\alpha, \quad k^\beta = \left(\frac{\pi}{2a}, -\frac{\pi}{2a} \right), \quad k^{\beta'} = -k^\beta$$

Hole fields

$$\psi_+^f(x) = \frac{1}{\sqrt{2}} [\psi_+^{k^f}(x) - \psi_+^{k^{f'}}(x)], \quad \psi_-^f(x) = \frac{1}{\sqrt{2}} [\psi_-^{k^f}(x) + \psi_-^{k^{f'}}(x)]$$

Nonlinear realization of the $SU(2)_s$ symmetry

$$u(x)\vec{e}(x) \cdot \vec{\sigma} u(x)^\dagger = \sigma_3, \quad u_{11}(x) \geq 0$$

Under $SU(2)_s$ the diagonalizing field $u(x)$ transforms as

$$u(x)' = h(x)u(x)g^\dagger, \quad u_{11}(x)' \geq 0,$$

$$h(x) = \exp(i\alpha(x)\sigma_3) = \begin{pmatrix} \exp(i\alpha(x)) & 0 \\ 0 & \exp(-i\alpha(x)) \end{pmatrix} \in U(1)_s$$

The composite vector field

$$v_\mu(x) = u(x)\partial_\mu u(x)^\dagger = iv_\mu^a(x)\sigma_a, \quad v_\mu^\pm(x) = v_\mu^1(x) \mp iv_\mu^2(x)$$

transforms as

$$v_\mu^3(x)' = v_\mu^3(x) - \partial_\mu\alpha(x), \quad v_\mu^\pm(x)' = \exp(\pm 2i\alpha(x))v_\mu^\pm(x)$$

Transformation rules of fermion fields

$$\begin{aligned}
 SU(2)_s : \quad & \psi_{\pm}^f(x)' = \exp(\pm i\alpha(x))\psi_{\pm}^f(x), \\
 U(1)_Q : \quad & {}^Q\psi_{\pm}^f(x) = \exp(i\omega)\psi_{\pm}^f(x), \\
 D_i : \quad & {}^{D_i}\psi_{\pm}^f(x) = \mp \exp(ik_i^f a) \exp(\mp i\varphi(x))\psi_{\mp}^f(x), \\
 O : \quad & {}^O\psi_{\pm}^{\alpha}(x) = \mp\psi_{\pm}^{\beta}(Ox), \quad {}^O\psi_{\pm}^{\beta}(x) = \psi_{\pm}^{\alpha}(Ox), \\
 R : \quad & {}^R\psi_{\pm}^{\alpha}(x) = \psi_{\pm}^{\beta}(Rx), \quad {}^R\psi_{\pm}^{\beta}(x) = \psi_{\pm}^{\alpha}(Rx)
 \end{aligned}$$

Leading terms in the effective Lagrangian for holes

$$\begin{aligned}
 \mathcal{L} = & \sum_{\substack{f=\alpha,\beta \\ s=+,-}} \left[M\psi_s^{f\dagger}\psi_s^f + \psi_s^{f\dagger}D_t\psi_s^f + \Lambda(\psi_s^{f\dagger}v_1^s\psi_{-s}^f + \sigma_f\psi_s^{f\dagger}v_2^s\psi_{-s}^f) \right. \\
 & \left. + \frac{1}{2M'}D_i\psi_s^{f\dagger}D_i\psi_s^f + \sigma_f\frac{1}{2M''}(D_1\psi_s^{f\dagger}D_2\psi_s^f + D_2\psi_s^{f\dagger}D_1\psi_s^f) \right]
 \end{aligned}$$

Covariant derivative coupling to composite magnon gauge field

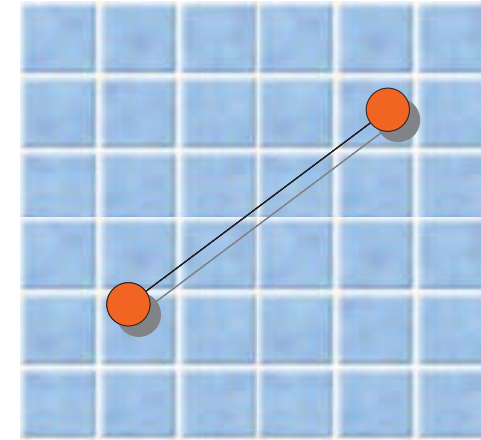
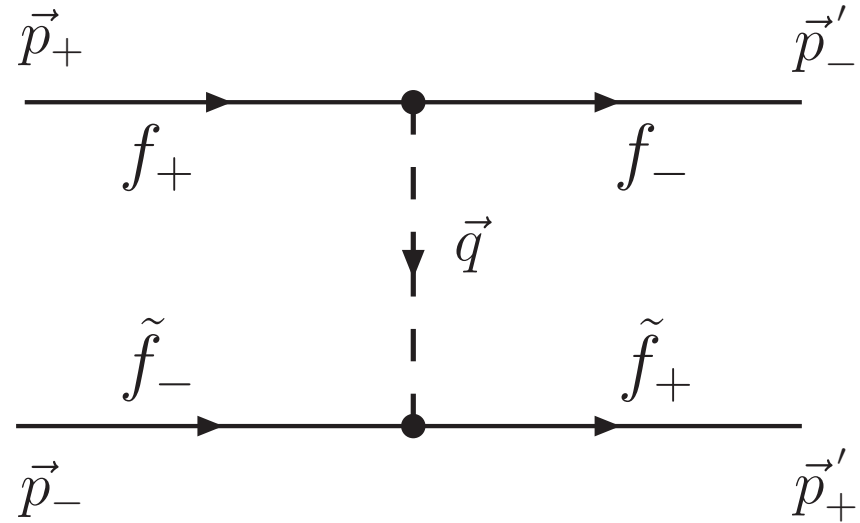
$$D_{\mu}\psi_{\pm}^f(x) = [\partial_{\mu} \pm i\nu_{\mu}^3(x)] \psi_{\pm}^f(x)$$

Shraiman, Siggia (1988); Wen (1989); Shankar (1989); Sushkov (1994); Brügger, Kämpfer, Moser, Pepe, UJW (2006)

Outline

Two-Hole States Bound by Magnon Exchange

Magnon exchange



One-magnon exchange potentials

$$V^{\alpha\alpha}(\vec{r}) = \gamma \frac{\sin(2\varphi)}{r^2}, \quad V^{\beta\beta}(\vec{r}) = -\gamma \frac{\sin(2\varphi)}{r^2},$$

$$V^{\alpha\beta}(\vec{r}) = V^{\beta\alpha}(\vec{r}) = \gamma \frac{\cos(2\varphi)}{r^2}, \quad \gamma = \frac{\Lambda^2}{2\pi\rho_s}$$

Two-hole Schrödinger equation for an $\alpha\beta$ pair

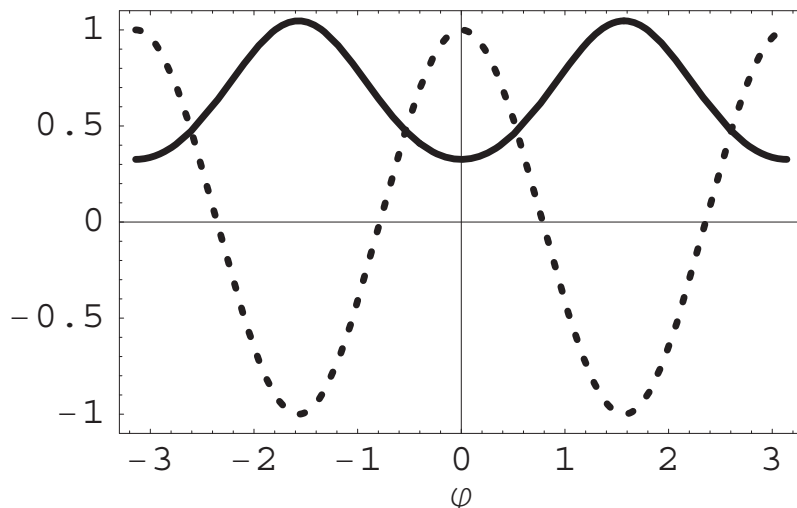
$$\begin{pmatrix} -\frac{1}{M'}\Delta & V^{\alpha\beta}(\vec{r}) \\ V^{\alpha\beta}(\vec{r}) & -\frac{1}{M'}\Delta \end{pmatrix} \begin{pmatrix} \Psi_1(\vec{r}) \\ \Psi_2(\vec{r}) \end{pmatrix} = E \begin{pmatrix} \Psi_1(\vec{r}) \\ \Psi_2(\vec{r}) \end{pmatrix}$$

Making the ansatz

$$\Psi_1(\vec{r}) \pm \Psi_2(\vec{r}) = R(r)\chi_{\pm}(\varphi)$$

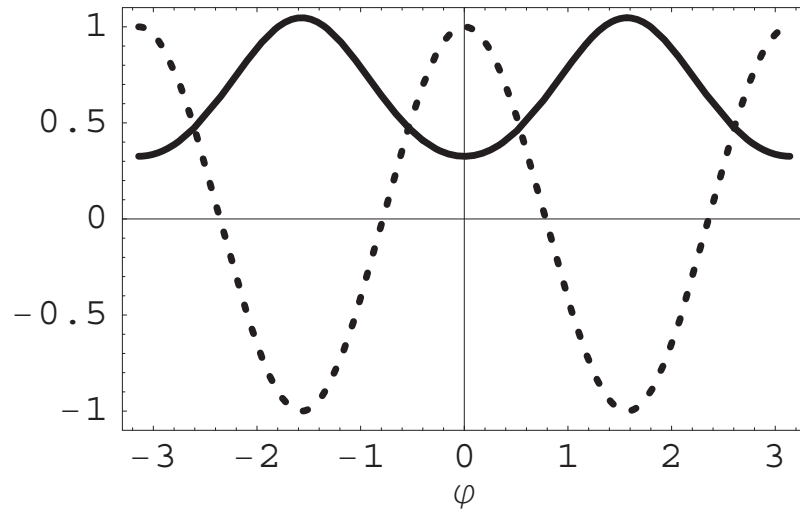
for the angular part of the wave function one obtains

$$-\frac{d^2\chi_{\pm}(\varphi)}{d\varphi^2} \pm M'\gamma \cos(2\varphi)\chi_{\pm}(\varphi) = -\lambda\chi_{\pm}(\varphi)$$

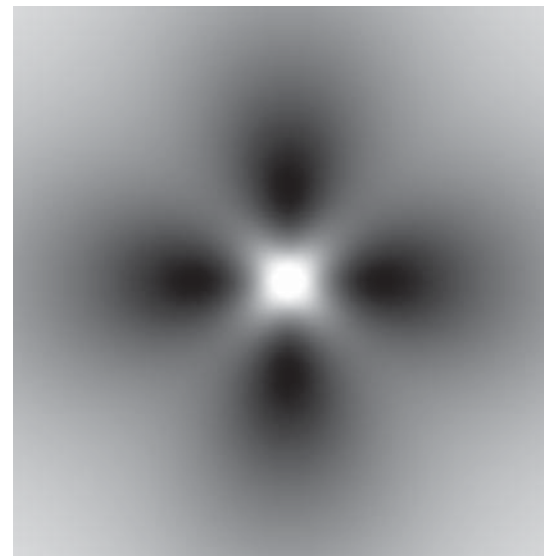


looks like s-wave,
but turns out to be p-wave

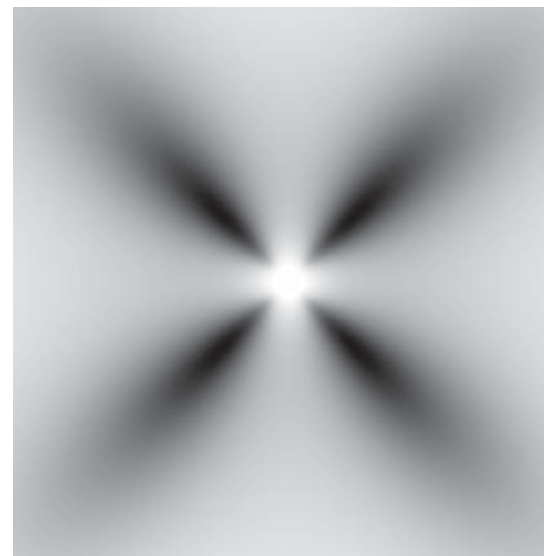
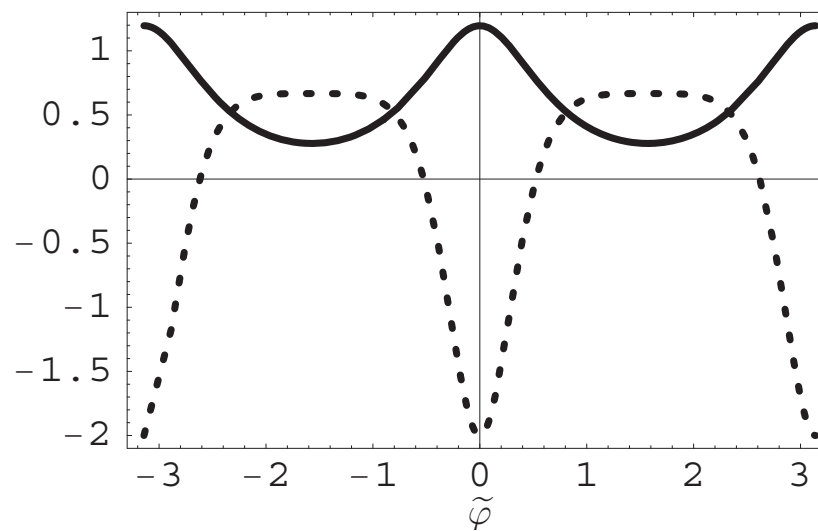
Two-hole bound states of $\alpha\beta$ and $\alpha\alpha$ pairs



Angular wave function



Probability density



Outline

Holes Localized on a Skyrmion

Topologically conserved current

$$j_\mu(x) = \frac{1}{8\pi} \varepsilon_{\mu\nu\rho} \vec{e}(x) \cdot [\partial_\nu \vec{e}(x) \times \partial_\rho \vec{e}(x)], \quad \partial_\mu j_\mu(x) = 0$$

Topological winding number

$$n[\vec{e}] = \int d^2x j_t = \frac{1}{8\pi} \int d^2x \varepsilon_{ij} \vec{e} \cdot [\partial_i \vec{e} \times \partial_j \vec{e}] \in \Pi_2[S^2] = \mathbb{Z},$$

Schwarz inequality for the energy

$$E[\vec{e}] = \int d^2x \frac{\rho_s}{2} \partial_i \vec{e} \cdot \partial_i \vec{e} \geq 4\pi \rho_s |n[\vec{e}]|$$

Selfduality condition

$$\partial_i \vec{e} + \varepsilon_{ij} \partial_j \vec{e} \times \vec{e} = 0$$

is satisfied by Skyrmion configurations

$$\vec{e}_{\rho,\gamma}(r, \chi) = \left(\frac{2r\rho}{r^2 + \rho^2} \cos(\chi + \gamma), \frac{2r\rho}{r^2 + \rho^2} \sin(\chi + \gamma), \frac{r^2 - \rho^2}{r^2 + \rho^2} \right)$$

Single-Hole-Skyrmion Hamiltonian

$$\begin{aligned}
H^f \Psi^f(r, \chi, \gamma) &= \begin{pmatrix} H_{++}^f & H_{+-}^f \\ H_{-+}^f & H_{--}^f \end{pmatrix} \begin{pmatrix} \Psi_+^f(x) \\ \Psi_-^f(x) \end{pmatrix} = E^f \Psi^f(x), \\
H_{++,--}^f &= -\frac{1}{2M'} \left[\partial_r^2 + \frac{1}{r} \partial_r - \frac{1}{r^2} \left(-i\partial_\chi \pm \frac{\rho^2}{r^2 + \rho^2} \right)^2 \right] \\
&\quad + \frac{1}{2\mathcal{I}(\rho)} \left(-i\partial_\gamma \mp \frac{\rho^2}{r^2 + \rho^2} \right)^2, \\
H_{+-}^{f*} &= H_{-+}^f = \sqrt{2}\Lambda\sigma_f \frac{\rho}{r^2 + \rho^2} \exp \left(i \left[2\chi + \gamma + \sigma_f \frac{\pi}{4} \right] \right)
\end{aligned}$$

Single-hole-Skyrmion wave function

$$\begin{aligned}
\Psi_{m_+, m_-, m}^f(r, \chi, \gamma) &= \\
\begin{pmatrix} \psi_+(r) \exp(i[m_+\chi - \sigma_f \frac{\pi}{8}]) \exp(i(m - \frac{1}{2})\gamma) \\ \sigma_f \psi_-(r) \exp(i[m_-\chi + \sigma_f \frac{\pi}{8}]) \exp(i(m + \frac{1}{2})\gamma) \end{pmatrix}
\end{aligned}$$

Two hole-Skyrmion wave function

$$\Psi_{m_+^\alpha, m_-^\alpha, m_+^\beta, m_-^\beta, m}^{\alpha\beta}(r_\alpha, \chi_\alpha, r_\beta, \chi_\beta, \gamma) = \begin{pmatrix} \psi_{++}(r_\alpha, r_\beta) \exp\left(i[m_+^\alpha \chi_\alpha + m_+^\beta \chi_\beta]\right) \exp(i(m-1)\gamma) \\ -\psi_{+-}(r_\alpha, r_\beta) \exp\left(i[m_+^\alpha \chi_\alpha + m_-^\beta \chi_\beta - \frac{\pi}{4}]\right) \exp(im\gamma) \\ \psi_{-+}(r_\alpha, r_\beta) \exp\left(i[m_-^\alpha \chi_\alpha + m_+^\beta \chi_\beta + \frac{\pi}{4}]\right) \exp(im\gamma) \\ -\psi_{--}(r_\alpha, r_\beta) \exp\left(i[m_-^\alpha \chi_\alpha + m_-^\beta \chi_\beta]\right) \exp(i(m+1)\gamma) \end{pmatrix}$$

90 degrees rotation of two-hole-Skyrmion ground state

$${}^O\Psi_{-1,1,-1,1,0}^{\alpha\beta}(r_\alpha, \chi_\alpha, r_\beta, \chi_\beta, \gamma) = -i\Psi_{-1,1,-1,1,0}^{\alpha\beta}(r_\alpha, \chi_\alpha, r_\beta, \chi_\beta, \gamma)$$

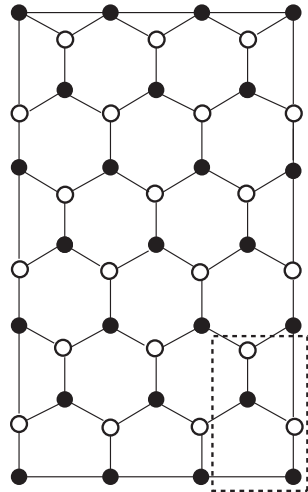
The bound state of two holes localized on a Skyrmion again has **p-wave symmetry** and is thus not a candidate for a preformed Cooper pair in a high-temperature superconductor.

Vlasii, Jiang, Hofmann, UJW, to appear

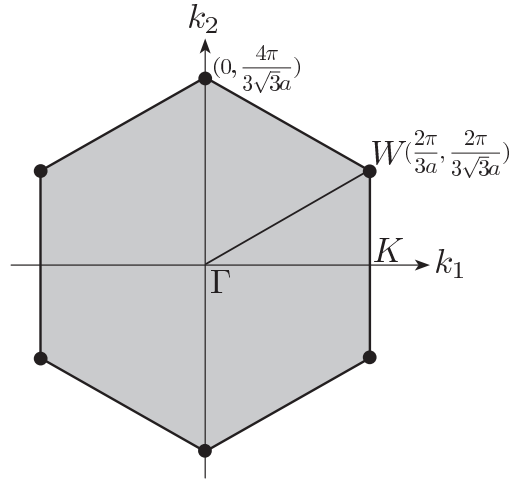
Outline

From Graphene to $\text{Na}_x\text{CoO}_2 \cdot y\text{H}_2\text{O}$

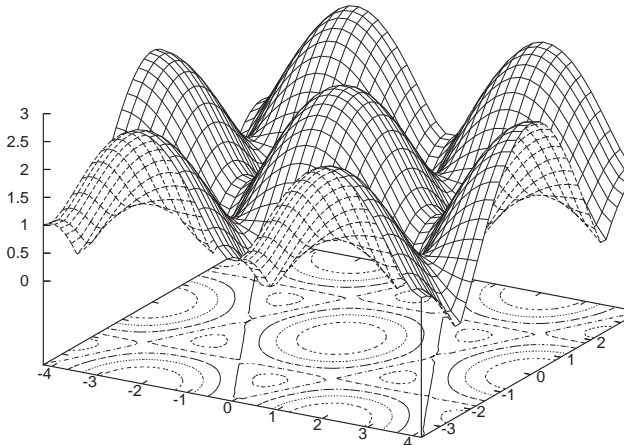
Hubbard model on the honeycomb lattice: Unbroken $SU(2)_s$ symmetric phase (graphene)



Honeycomb
lattice



Brillouin zone

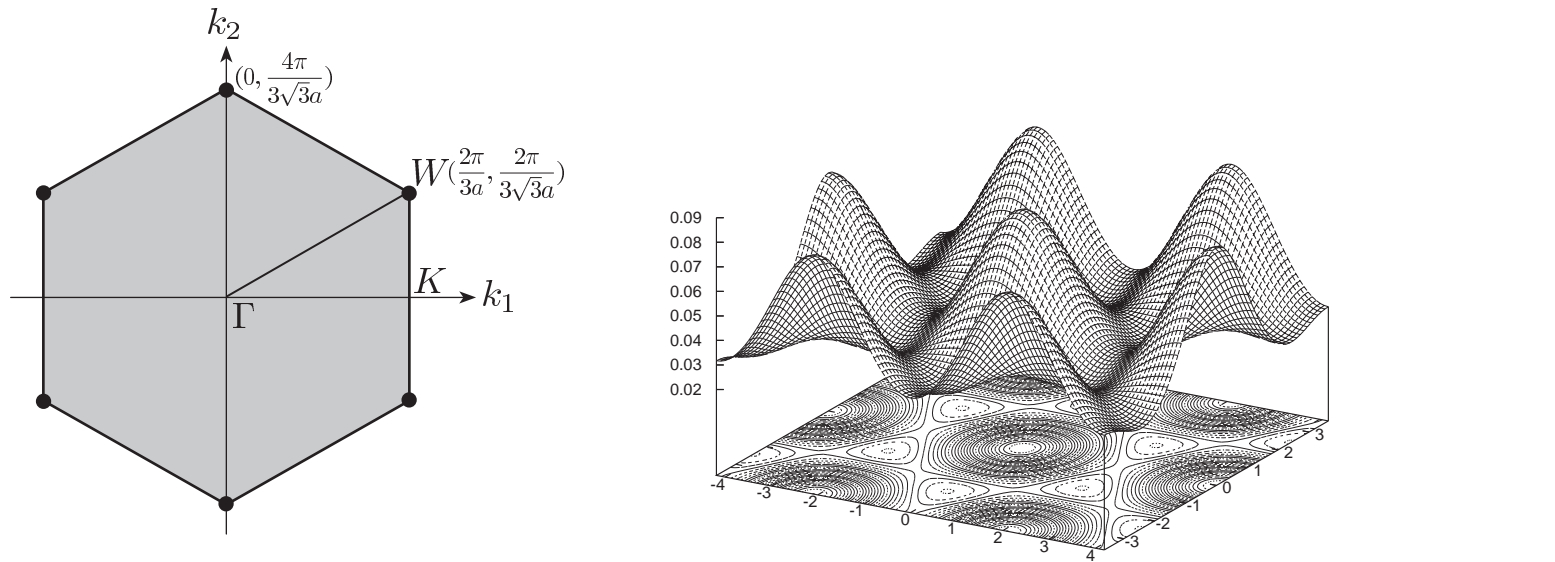


Dispersion relation

Effective Dirac Lagrangian for free graphene

$$\mathcal{L} = \sum_{\substack{f=\alpha,\beta \\ s=+,-}} \bar{\psi}_s^f \gamma_\mu \partial_\mu \psi_s^f$$

Hole dispersion in the t - J model ($\text{Na}_x\text{CoO}_2 \cdot y\text{H}_2\text{O}$)



Effective Lagrangian for Magnons and Holes

$$\begin{aligned} \mathcal{L} = & \sum_{\substack{f=\alpha,\beta \\ s=+,-}} \left[M \psi_s^{f\dagger} \psi_s^f + \psi_s^{f\dagger} D_t \psi_s^f + \frac{1}{2M'} D_i \psi_s^{f\dagger} D_i \psi_s^f \right. \\ & \left. + \Lambda \psi_s^{f\dagger} (i s v_1^s - \sigma_f v_2^s) \psi_{-s}^f \right] + \frac{\rho_s}{2} \left(\partial_i \vec{e} \cdot \partial_i \vec{e} + \frac{1}{c^2} \partial_t \vec{e} \cdot \partial_t \vec{e} \right) \end{aligned}$$

Conclusions

- Doped antiferromagnets are described quantitatively by systematic low-energy effective field theories for magnons and doped holes.
- Quantum Monte Carlo calculations using the loop-cluster algorithm yield the low-energy parameters with fraction of a per mille accuracy.
- After fixing the low-energy parameters, the Monte Carlo data provide a very high-accuracy quantitative test of the magnon effective theory.
- Through the Shraiman-Siggia coupling, magnon exchange binds hole pairs in the p-wave channel.
- Two holes localized on a Skyrmion again have p-wave symmetry, and thus are not a candidate for a preformed pair.
- Systems on the honeycomb lattice as well as electron-doped systems have been and are still being investigated with the same techniques.
- On the honeycomb lattice, two holes bound by magnon exchange have f-wave symmetry.